Kinematics of Spiral Waves in Excitable Media

Vladimir S. Zykov

Abstract Spiral waves rigidly rotating in excitable media sometimes play a constructive role in self-organization, while in many cases they cause an undesirable and dangerous activity. An understanding of spiral wave kinematics can help to control or to prevent this self-sustained activity. A description of the spiral wave kinematics performed by use of a free-boundary approach, reveals the selection principle which determines the shape and the rotation frequency of spiral waves in an unbounded medium with a given excitability. It is shown that a rigidly rotating spiral in a medium with strongly reduced refractoriness is supported within an excitability range restricted by two universal limits. At the low excitability limit, the spiral core radius diverges, while it vanishes at the high excitability limit and the spiral wave resembles the Yin-Yang pattern.

1 Introduction

An excitable medium can be considered as a population of active elements coupled locally through diffusion-like transport processes. Each individual active element is stable with respect to small external perturbations. However, it can be excited by the application of a super-threshold stimulus. Therefore, an excitation induced locally is able to propagate through the population of diffusively coupled elements as a self-sustained wave. After a recovery process, the medium returns to the resting state.

Rotating self-sustained spiral waves are among the most prominent examples of self-organized patterns in excitable media. They have been observed in systems of quite different nature like the social amoebae colonies [1] (see also chapter **Spiral Waves of the Chemo-Attractant cAMP Organise Multicellular Development**

V. S. Zykov (✉)
Max Planck Institute for Dynamics and Self-Organization, 37077 Göttingen, Germany
e-mail: vladzykov@googlemail.com

K. Tsuji and S. C. Müller (eds.), *Spirals and Vortices*,
The Frontiers Collection, https://doi.org/10.1007/978-3-030-05798-5_16

in the Social Amoebae), the chemical Belousov–Zhabotinsky (BZ) reaction [2] (chapter **Chemical Oscillation and Spiral Waves**), heart muscle [3] (chapter **Spiral Waves in the Heart**), the retina of the eye [4] (chapter **Yet More Spirals**), the oxidation of CO to CO_2 on platinum single crystal surfaces [5] (chapter **Shedding Light on Chaos**), yeast extracts during glycolysis [6] (chapter **Yet More Spirals**), and so on.

In the simplest case, the spiral rotates rigidly and its tip describes a circular orbit around the core [7, 8]. Varying the parameters of the midium one can effectively control the motion of spiral waves which can be used to destroy undesirable wave activity [9–12]. From this point of view the selection principles that determine the shape and the rotating frequency of spiral waves have to be understood.

From a mathematical point of view the main dynamical features of a broad class of excitable media can be simulated by a two-component reaction-diffusion system.

$$\frac{\partial u}{\partial t} = D\Delta u + F(u, v), \tag{1}$$

$$\frac{\partial v}{\partial t} = D_v \Delta v + \varepsilon G(u, v). \tag{2}$$

Here the local kinetics of an activator u and an inhibitor v is specified by the nonlinear functions $F(u, v)$ and $G(u, v)$. The diffusion coefficients D, D_v and the small multiplier ε are important control parameters. They are universal and applicable to a broad variety of models (see chapter **Reaction-Diffusion Patterns and Waves.**

From the experimental point of view, there is also some universality because there are many common kinematical features of spiral waves observed in quite different chemical and biological excitable media.

In this chapter we concentrate on an approximation of the reaction-diffusion model, as indicated in Eqs. 1 and 2, that allows us to reach a deeper understanding of the kinematical features of spiral waves. In the framework of this approach we are interested mostly in the motion of the boundary restricting an excited region. We will show that this so-called free-boundary approach essentially simplifies and generalizes the theoretical consideration of the spiral wave dynamics. Simultaneously, this approach helps us to reveal such important medium parameters, which can be measured experimentally.

2 Two First Steps Towards Spiral Wave Kinematics

In their seminal theoretical work, Wiener and Rosenblueth [13] showed in 1946 that the self-sustained activity in the cardiac muscle can be associated with an excitation wave rotating around an obstacle. In particular, they considered a motion of a wave rotating around a round obstacle as shown in Fig. 1a. In this very simplified kinematical model, they assumed that an excited part of the propagating wave is restricted by a very thin boundary consisting of a wave front (thick solid) and a wave back (thin

solid). It was also assumed that all points of the boundary are moving in the normal direction at the same velocity $c_n = const$. If the radius of the circular obstacle is given as R, the rotational frequency of the spiral wave should be $\omega = 2\pi R/c_n$. The shape of the wave front is also well determined in this case and represents the involute of the obstacle boundary. It means that the length of the interval AB of a tangent is equal to the arc length AC (see chapter **Spirals, Their Types and Peculiarities**). The wave back following the wave front has the same shape if turned around the rotational center by the angle ωd_u, where d_u is the duration of the excited state.

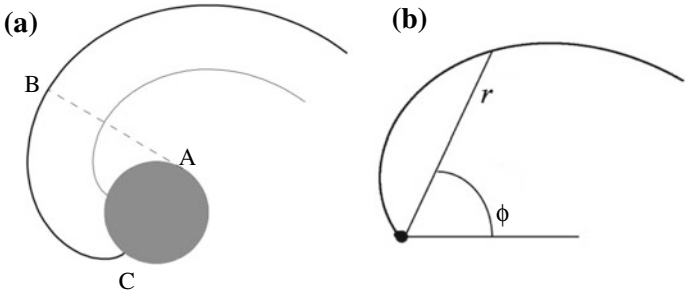

Fig. 1 Two examples of spiral wave kinematics. **a** Spiral wave rotating around a round unexcitable obstacle (dark region). **b** Top view on a screw dislocation growing on a crystal surface

A second important example shown in Fig. 1b represents the shape of a screw dislocation growing on a crystal surface [14]. In contrast to the first example, the authors assumed that the normal velocity of the wave front is not a constant, but strongly depends on the front curvature, namely

$$c_n = c_p - Dk, \tag{3}$$

where c_p is the velocity of a planar front and k is its curvature. In the modern literature this relationship has obtained the name eikonal equation (see chapter **Chemical Oscillations and Spiral Waves**). Note, that in this case the wave front is rotating around a central point. In the vicinity of this point the front velocity c_n vanishes, and the front curvature reaches the value c_p/D in accordance with Eq. 3. The shape of the wave front is suitably expressed in the polar coordinates (r, ϕ) with the origin at the rotational center

$$x = r\cos[\phi(r) - \omega r], \;\; y = r\sin[\phi(r) - \omega r], \tag{4}$$

where ω is the rotational frequency of the wave front.

A detailed numerical analysis has shown that an acceptable solution $\phi(r)$ of Eqs. 3 and 4 does exist only for a single value of the rotational frequency

$$\omega = 0.331 c_p^2/D. \tag{5}$$

It is important that both shapes of the spiral wave fronts shown in Fig. 1 are approaching the Archimedean spiral far away from the rotational center.

3 Free Boundary Approach

The next relevant step in the understanding of the spiral wave kinematics has been done by Pelcé and Sun [15]. They recognized that in both cases mentioned in Sect. 2 the wave front kinematics is completely independent of the wave back motion. In contrast to this the wave front and the wave back are usually interacting with each other. It can be clearly seen in Fig. 2, where a snapshot of a counterclockwise rotating spiral is shown. This picture resembles a typical pattern of spiral wave rotating within a homogeneous chemical or biological medium around a core of finite size (see chapter **Reaction-Diffusion Patterns and Waves**).

At one part of the excited state boundary the activator u is growing ($du/dt > 0$) that corresponds to the wave front. At another part of the boundary $du/dt < 0$ that corresponds to the wave back. These two parts meet each other at a so-called phase change point [16]. This point q describes a circular pathway around the circulation center, which represents the spiral wave core.

Another interesting point Q is located at the place, where the radial direction is a tangent to the excited state boundary. Here the normal front velocity is orthogonal to the radial direction and, hence, the point Q also describes a circular pathway around the circulation center.

The kinematics of the wave front and the wave back are closely connected and should be considered in parallel. To this aim it is very useful to describe the boundary of the excited state by the so-called natural equation which determines the boundary curvature k as a function of the arc length s counted from the phase change point q [17, 18].

Then the Cartesian coordinates $x(s)$, $y(s)$ of the boundary and the angle $\Theta(s)$ which determines the normal direction obey the obvious equations:

$$\Theta(s) = \Theta(0) - \int_0^s k(s')ds', \tag{6}$$

$$x(s) = x(0) + \int_0^s \cos(\Theta(s'))ds', \tag{7}$$

$$y(s) = y(0) + \int_0^s \sin(\Theta(s'))ds'. \tag{8}$$

During the boundary rotation, each of its point is moving at the velocity ωr around the rotational center. This velocity can be represented as a sum of a normal velocity $c_n(s)$ (orthogonal to the boundary) and the tangential velocity $c_\tau(s)$ (along the boundary), as drawn in Fig. 3. It was shown that for a rigidly rotating spiral these two velocities and $k(s)$ obey the following system of differential equations [17]

$$\frac{dc_n}{ds} = \omega + kc_\tau, \tag{9}$$

$$\frac{dc_\tau}{ds} = -kc_n. \tag{10}$$

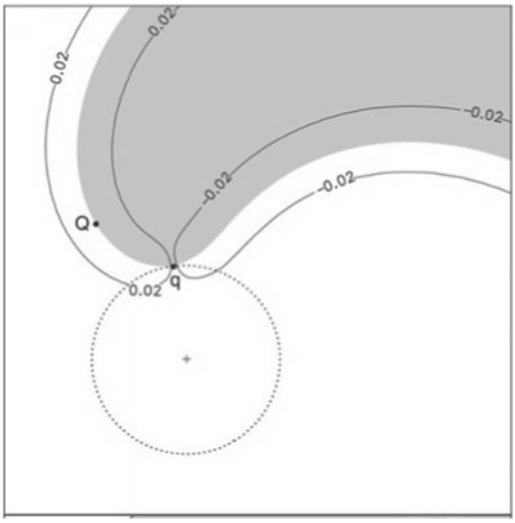

Fig. 2 Spiral wave rotating around a circular core. The shaded region corresponds to an excited state. The dotted line depicts the trajectory of the phase change point q rotating around the circulation center (+). Solid lines indicate isolines of the temporal derivative du/dt of the activator. Taken from [18]

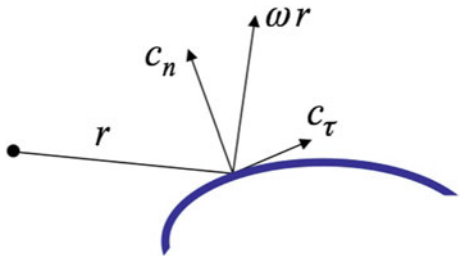

Fig. 3 Normal velocity c_n and tangential velocity c_τ of a rotating boundary

After rescaling ($S = sc_p/D, R = rc_p/D, C = c/c_p, K = Dk/c_p, \Omega = \omega D/c_p^2$), Eqs. 9 and 10 transform into the dimensionless form

$$\frac{dC_n}{dS} = \Omega + KC_\tau, \tag{11}$$

$$\frac{dC_\tau}{dS} = -KC_n. \tag{12}$$

Equations 11 and 12 are the result of a pure kinematical consideration. To describe the boundary shape of a spiral wave rotating in an excitable medium, this system should be supplemented by the eikonal equation describing the velocity-curvature relationship written in dimensionless form in accordance with Eq. 3 as

$$C_n^+ = 1 - K^+. \tag{13}$$

The phase portrait of Eqs. 11–13 computed for $\Omega = 0.1333$ is shown in Fig. 4. A trajectory describing the wave front starts at the line, where $C_n^+(0) = 0$ and $0 \le C_\tau(0) \le 1$. In Fig. 4 three trajectories of the system computed for different $C_t \equiv C_\tau(0)$ are shown. At the beginning of all trajectories C_n^+ increases and

C_τ^+ decreases. However, the normal velocity C_n^+ reaches a maximum and starts to decrease along the trajectory computed for $C_t = 0.3$. Moreover, this trajectory includes a part, where $C_n^+ < 0$, which contradicts the definition of a wave front. The trajectory crosses the line $C_n = 0$ again at $C_\tau \approx 0.61$. This point can be considered as the starting point of a separate, fourth trajectory, which firstly crosses the line $C_n = 1$ and then approaches the nullcline $C_n = 1 + \Omega/C_\tau$ for $C_\tau \to \infty$.

The trajectory computed for $C_t = 0.5$ crosses the line $C_\tau = 0$ twice and also approaches the nullcline $C_n = 1 + \Omega/C_\tau$ for $C_\tau \to \infty$.

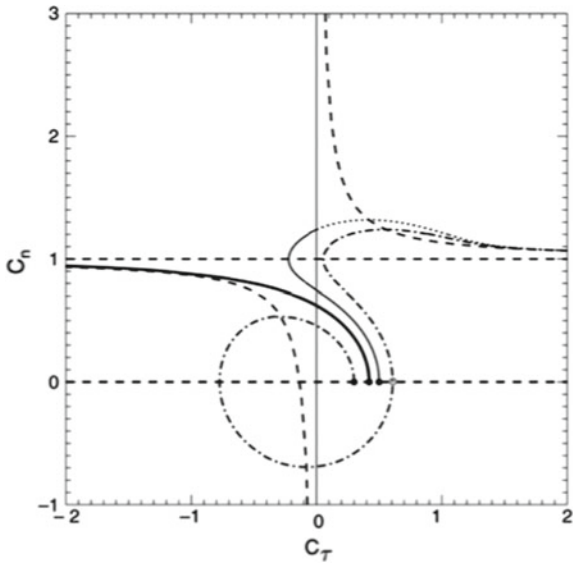

Fig. 4 The phase portrait of the free-boundary equations (Eqs. 11–13) corresponding to $\Omega = 0.1333$. Dashed lines show nullclines of the system ($dC_n/dS = 0$ and $dC_\tau/dS = 0$). Black dots mark starting points of the trajectories computed for different values of $C_t \equiv C_\tau(0)$. Dash-dotted line corresponds to $C_t = 0.3$, thick solid is obtained for $C_t = 0.42055$. The first part of the trajectory computed for $C_t = 0.5$ is depicted by a thin solid line and the following part is shown by dotted line. Taken from [18]

The front shapes corresponding to these two trajectories ($C_t = 0.3$ and $C_t = 0.5$) are shown in Fig. 5a. They are obtained by substitution of the computed function $K(s)$ into Eqs. 6–8 with $\Theta(0) = \pi/2$, $X(0) = 0$, and $Y(0) = C_t/\Omega$. It can be seen that the trajectory starting at $C_t = 0.3$ (dash-dotted line) has no physical sense. Another trajectory, corresponding to $C_t = 0.5$, contains a part depicted by thin solid, which can be considered as a front of a wave rotating within a disk of radius R_D with a no-flux boundary. The first intersection of this trajectory with the line $C_\tau = 0$ corresponds to the point Q. The second intersection occurs at the disk boundary, where $C_n^+ = \Omega R_D$. The part of the trajectory outside the disk of radius R_D does not match any rotating waves in excitable media. It resembles antispirals [19] or twisted spirals [20] observed in oscillatory media.

By starting at $C_t = 0.5$ and continuously decreasing C_t one can compute trajectories corresponding to an increasing disk radius R_D. The limiting case $R_D \to \infty$ is obtained for $C_t = 0.42055$ and is shown in Fig. 5b by the thick solid line. The corresponding trajectory is presented in Fig. 4 by the thick solid. Obviously, this solution of Eqs. 11–13 represents a spiral wave front in an unbounded medium rotating at the

given angular velocity Ω. Asymptotics of this solution for $S \to \infty$ can be specified as in [17]

$$C_n^+(\infty) = 1, \quad C_\tau^+(S) = \sqrt{2\Omega S}, \quad K(S) = \sqrt{\frac{\Omega}{2S}}. \tag{14}$$

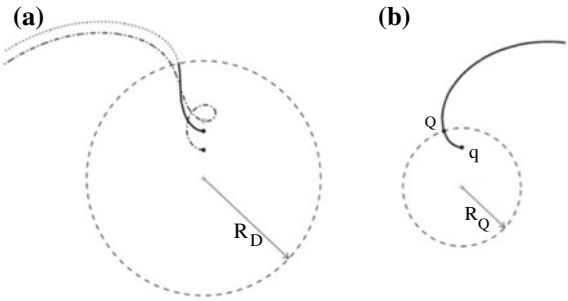

Fig. 5 Wave front shapes corresponding to the trajectories shown in Fig. 4. **a** Front shapes computed for $C_t = 0.3$ (dash-dotted line) and $C_t = 0.5$ (thin solid and dotted lines). **b** Front shape obtained for $C_t = 0.42055$. Taken from [18]

A repetition of similar computations for different values of Ω reveals a unique relationship $\Omega = \Omega(C_t)$ depicted in Fig. 6. Here C_t varies within the whole physically available range $0 \le C_t \le 1$. The angular velocity Ω vanishes at $C_\tau = 1$. This limiting case corresponds to the low excitability limit studied in [21], where an analytical expression $\Omega = 0.198(1 - C_t)^{3/2}$ has been derived. This expression shown by the dotted line in Fig. 6 approximates very well the relation found numerically for $C_t \approx 1$. However, it strongly deviates from numerical data obtained for small C_t.

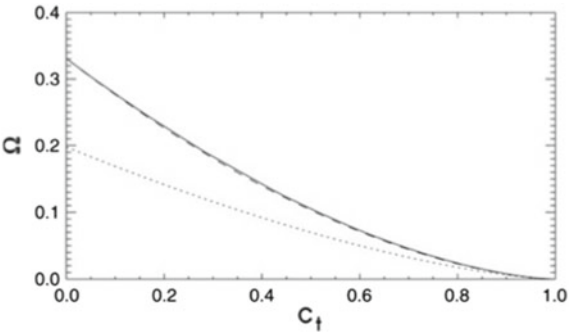

Fig. 6 Angular velocity Ω of a wave front as a function of the tangential velocity C_t of the spiral tip. The dashed line depicts the approximation given by Eq. 15. The dotted line corresponds to the asymptotic found in [21] specified by the first term in Eq. 15. Taken from [18]

In another limiting case, the value $\Omega = 0.331$ computed for $C_t = 0$ coincides with the result obtained firstly by Burton, Cabrera and Frank [14] for screw dislocations growing on crystal surface (see chapter **Appearance in Nature**) and reproduced later many times [17, 21, 22].

The suitable approximation of the relationship $\Omega(C_t)$ obtained numerically for the whole range $0 \le C_t \le 1$ reads

$$\Omega = 0.198(1 - C_t)^{3/2} + 0.133(1 - C_t)^2. \tag{15}$$

It supplies a nice accuracy within the whole range $0 \leq C_t \leq 1$, as can be seen in Fig. 6.

Thus, the front shape of a rigidly rotating spiral wave and its angular velocity Ω are uniquely determined by the tangential velocity C_t of the spiral tip.

The results obtained for the wave front have to be used to integrate Eqs. 11 and 12 for the spiral wave back taking into account that during the excited state, the inhibitor value is increasing from $v = v^+$ at the wave front till $v = v^-$ at the wave back. The value v^- of the inhibitor at the wave back can be found from Eq. 2 under the assumption that the value $G(u_e(v), v)$ remains practically constant and equal to G^* during the excited state. Note that for many systems under consideration, e.g. cardiac tissue, the inhibitor diffusion $D_v = 0$, which simplifies the analysis.

Since the pattern is rotating at a constant angular velocity ω, the value of the inhibitor near the wave back is expressed in accordance with Eq. 2 as

$$v^-(R) = v^+ + \frac{G^*\varepsilon}{\omega}[\gamma^+(R) - \gamma^-(R)], \tag{16}$$

where γ^+ and γ^- specify the location of the front and the back, respectively, as shown in Fig. 7. The thick solid line in Fig. 7 represents the front of the rotating wave computed for a given value of $\Omega = 0.1333$. The front curvature $K(s)$ obtained during these computations has to be substituted into Eqs. 6–8 in order to determine the front shape in the Cartesian and polar coordinates.

The inhibitor v^- strongly affects the normal propagation velocity. In order to reflect this fact, the eikonal equation (Eq. 3) should be modified to

$$c_n^- = c_p(v^-) - Dk. \tag{17}$$

Substituting the value v^- expressed by Eq. 16 into Eq. 17 we get after rescaling

$$C_n^- = 1 - K^- - \frac{B}{\Omega}[\gamma^+(R) - \gamma^-(R)]. \tag{18}$$

The multiplier B appearing in this dimensionless expression is a very important control parameter and reads as

$$B = \frac{2D}{c_0^2 d_u}. \tag{19}$$

In order to obtain the shape of the wave back Eqs. 11–12 and 18 have to be integrated in the reverse arclength direction starting at $S = 0$ with initial conditions $C_n^-(0) = 0$ and $C_\tau^-(0) = C_t$. The obtained values of $K^-(S)$ have to be substituted into Eqs. 6–8 with $\Theta(0) = \pi/2$, $X(0) = 0$, and $Y(0) = C_t/\Omega$ in order to determine the dependence $\gamma^-(R)$.

It is important to emphasize that the shape of the wave back is strongly depended on the parameter B as shown in Fig. 7. It is expected for a physically correct solution that the derivatives $d\gamma^-/dS$ and dR^-/dS are positive. If B is relatively small, the derivative $d\gamma^-/dS$ vanishes at some S and becomes negative (see dotted line). If B

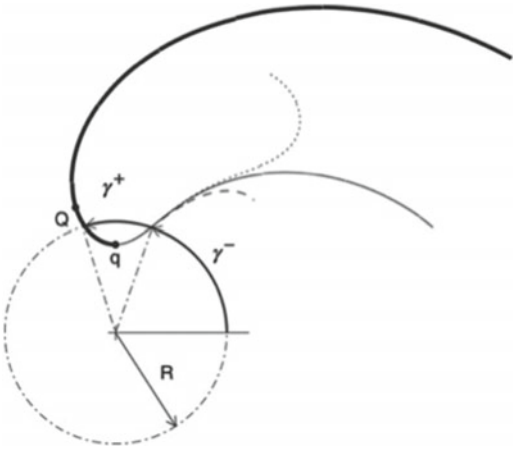

Fig. 7 Spiral wave shape obtained for $\Omega = 0.1333$. The front shape corresponds to Fig. 5b. The back shape is computed from Eqs. 11, 12, and 18 for different values of the dimensionless parameter B. Dotted and dashed lines correspond to $B = 0.2971$ and $B = 0.3008$, respectively. Thin solid line corresponds to $B = 0.2979$ found by a trial and error method. Taken from [18]

is relatively large, the derivative dR^-/dS vanishes (see dashed line). Using a trial and error method, one must vary the value of B trying to obtain the solution with the asymptotic $C_n^-(-\infty) = -1$.

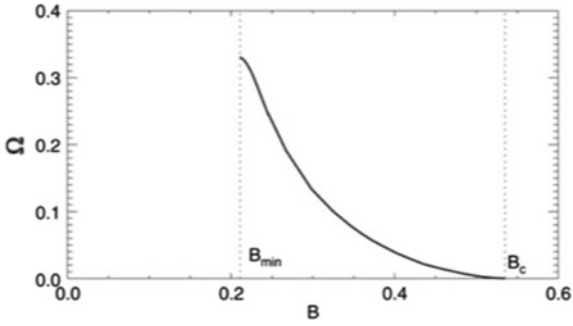

Fig. 8 The dimensionless angular velocity of a rigidly rotating spiral $\Omega = \Omega_{FB}(B)$ selected as a solution of the free-boundary problem based on Eqs. 11–13, and 18 versus the dimensionless parameter B characterizing the excitability of the medium. Taken from [18]

Thus, the obtained solution of the free-boundary problem for a spiral wave in an unbounded medium is uniquely determined by the value of the dimensionless parameter B for a given value of the angular velocity Ω. Repetition of these computations for different values of Ω from the interval $0 < \Omega < 1$ yields the universal relationship $\Omega = \Omega(B)$ shown in Fig. 8.

4 Two Limiting Cases

There are two limiting cases which characterize the relationship shown in Fig. 8. Firstly, our computations show that the highest angular velocity $\Omega = 0.331$ is reached at $B = B_{min} \approx 0.211$. Secondly, it is known that an undamped excitation wave in

a two-dimensional medium is supported only if $B < B_c \approx 0.535$ [23–25]. Hence, in a medium with a strongly reduced refractoriness a rigidly rotating spiral can be obtained only within the interval $B_{min} < B < B_c$.

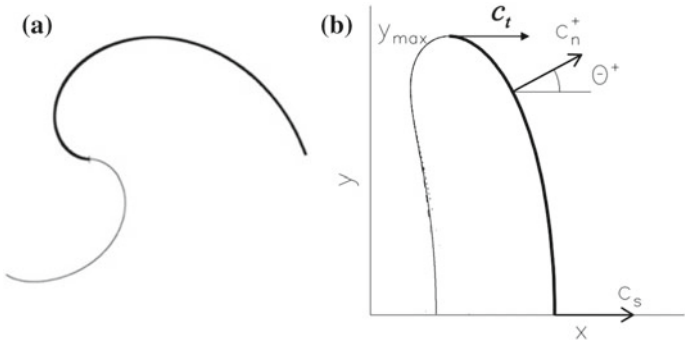

Fig. 9 The solution of the free-boundary problem Eqs. 11–13 and 18 corresponding to the limiting cases **a** $B = B_{min}$ and **b** $B = B_c$

The solution of the free-boundary problem obtained for $B = B_{min}$ is illustrated in Fig. 9a. Comparing Figs. 9a and 7 one can conclude that in this limiting case the point Q coincides with the spiral tip q, and they both are located at the rotation center. The radius of the spiral tip trajectory, $R_q = C_t/\Omega$, vanishes in the limit $B = B_{min}$. The curvature K_Q reaches the maximum $K_Q = 1$. The shape of the wave front is identical to that obtained by Burton, Cabrera and Frank [14]. The shape of the wave back reproduces the front shape, except for the immediate vicinity of the spiral tip. The wave back is turned by angle π with respect to the front, and the Cartesian coordinates of the wave boundary and their first derivatives are smooth functions of the arc length. In fact, in this limit the spiral wave form approaches the Yin-Yang pattern.

In the second limiting case, $B = B_c$, the angular velocity vanishes and the radius of the spiral wave core diverges. The shape of the spiral wave approaches the critical finger first studied in [23] and illustrated in Fig. 9b. The boundary of the excited region shown here undergoes a translational motion along the X axis at a constant velocity. Obviously, this velocity should be equal to the velocity c_p of a planar wave.

Thus, in a medium with a strongly reduced refractoriness the dimensionless angular velocity Ω is a unique monotonously decreasing function of the dimensionless parameter B. This function $\Omega = \Omega(B)$ changes between 0.331 and zero within the interval $B_{min} < B < B_c$. The radius of the spiral tip trajectory vanishes at $B = B_{min}$ and diverges at $B = B_c$.

5 Concluding Remarks

In this chapter we have demonstrated that the free-boundary approach allows us to clarify the basic principles of spiral wave selection in excitable media. It is shown that the rotational frequency and the spiral core radius in a medium with a short refractoriness are completely determined by a single dimensionless parameter B determined by Eq. 19. The value of this parameter can be estimated numerically or even analytically for quite different mathematical models. Moreover, it can be obtained as a result of direct experimental measurements.

However, the kinematical description of the rigidly rotating spiral waves represented in this work is, in fact, only an important limiting case of a much more complicated problem. As an example, three very important tasks, which should be solved in the near future are listed below.

First of all, note that the propagation velocity of a stationary propagating wave front is a nonlinear function of the front curvature [17]. A linear eikonal equation (Eq. 3) can be obtained only for $\varepsilon = 0$. For any $\varepsilon > 0$ there is a critical value of the front curvature K_{cr}, which restricts the region, where undamped wave propagation is supported. Point Q (see Fig. 7) is in stationary movement along a circular trajectory. The wave front at this point is curved and its curvature cannot exceed K_{cr}. This also restricts the angular velocity of a spiral wave [17]. This circumstance should be taken into account, when a medium with $B \approx B_{min}$ is considered [18].

Another very important issue is, of course, the role of the refractoriness of the medium. This problem is currently not solved. An important step in this direction is a recently developed kinematical description of a periodic sequence of the wave segments [26].

Finally, the described kinematical theory is applicable to so-called trigger-trigger waves [22]. However, under corresponding parameter variations, these waves can be transformed to so-called trigger-phase waves [27–29]. Moreover, there is a continuous transition between these two types of spiral kinematics [30], which should be studied in detail.

Thus, the kinematical theory of spiral waves represents a very interesting and intensively growing field for future investigations aimed, e.g., to find out efficient ways to prevent or to suppress an undesirable and dangerous self-sustained wave activity in excitable media.

References

1. G. Gerisch, Periodische Signale steuern die Musterbildung in Zellverbänden. Naturwissenschaften **58**, 430–438 (1971)
2. A.T. Winfree, Spiral waves of chemical activity. Science **175**, 634–636 (1972)
3. M.A. Allessie, F.I.M. Bonke, F.J.G. Schopman, Circus movement in rabbit atrial muscle as a mechanism of tachycardia. Circ. Res. **33**, 54–62 (1973)
4. N.A. Gorelova, J. Bures, Spiral waves of spreading depression in the isolated chicken retina. J. Neurobiol. **14**, 353–363 (1983)

5. S. Jakubith, H.H. Rotermund, W. Engel, A. von Oertzen, G. Ertl, Spatiotemporal concentration patterns in a surface reaction: propagating and standing waves, rotating spirals, and turbulence. Phys. Rev. Lett. **65**, 3013–3016 (1990)
6. T. Mair, S.C. Müller, Traveling NADH and proton waves during oscillatory glycolysis in vitro. J. Biol. Chem. **271**, 627–630 (1996)
7. S.C. Müller, T. Plesser, B. Hess, The structure of the core of the spiral wave in the Belousov-Zhabotinskii reaction. Science **230**, 661–663 (1985)
8. G.S. Skinner, H.L. Swinney, Periodic to quasiperiodic transition of chemical spiral rotation. Physica D **48**, 1–16 (1991)
9. K.I. Agladze, V.A. Davydov, A.S. Mikhailov, An observation of resonance of spiral waves in distributed excitable medium. JETP Lett. **45**, 601–603 (1987)
10. O. Steinbock, V.S. Zykov, S.C. Müller, Control of spiral-wave dynamics in active media by periodic modulation of excitability. Nature **366**, 322–324 (1993)
11. V.N. Biktashev, A. Holden, Design principles of a low voltage cardiac defibrillator based on the effect of feedback resonant drift. J. Theor. Biol. **169**, 101–112 (1994)
12. A.V. Panfilov, S.C. Müller, V.S. Zykov, J.P. Keener, Elimination of spiral waves in cardiac tissue by multiple electrical shocks. Phys. Rev. E **61**, 4644–4647 (2000)
13. N. Wiener, A. Rosenblueth, The mathematical formulation of the problem of conduction of impulses in a network of connected excitable elements, specifically in cardiac muscle. Arch. Inst. Cardiol. de Mex. **16**, 205–265 (1946)
14. W.K. Burton, N. Cabrera, F.C. Frank, The growth of crystals and the equilibrium structure of their surfaces. Philos. Trans. R. Soc. Lond. Ser. A **243**, 299–358 (1951)
15. P. Pelcé, J. Sun, Wave front interaction in steadily rotating spirals. Physica D **48**, 353–366 (1991)
16. F.B. Gul'ko, A.A. Petrov, Mechanism of formation of closed propagation pathways in excitable media. Biofizika **17**, 261–270 (1972)
17. V.S. Zykov, *Simulation of Wave Processes in Excitable Media* (Manchester University Press, Manchester, 1987)
18. V.S. Zykov, Kinematics of rigidly rotating spiral waves. Physica D **238**, 931–940 (2009)
19. I. Aranson, L. Kramer, The world of the complex Ginzburg-Landau equation. Rev. Mod. Phys. **74**, 99–143 (2002)
20. O. Rudzik, A.S. Mikhailov, Front reversals, wave traps, and twisted spirals in periodically forced oscillatory media. Phys. Rev. Lett. **96**, 018302 (2006)
21. V. Hakim, A. Karma, Theory of spiral wave dynamics in weakly excitable media: asymptotic reduction to a kinematic model and applications. Phys. Rev. E **60**, 5073–5105 (1999)
22. J.J. Tyson, J. Keener, Singular perturbation theory of traveling waves in excitable media (a review). Physica D **32**, 327–361 (1988)
23. A. Karma, Universal limit of spiral wave propagation in excitable media. Phys. Rev. Lett. **66**, 2274–2277 (1991)
24. V.S. Zykov, K. Showalter, Wave front interaction model of stabilized propagating wave segments. Phys. Rev. Lett. **94**, 068302 (2005)
25. A. Kothe, V.S. Zykov, H. Engel, Second universal limit of wave segment propagation in excitable media. Phys. Rev. Lett. **103**, 154102 (2009)
26. V.S. Zykov, E. Bodenschatz, Periodic sequence of stabilized wave segments in an excitable medium. Phys. Rev. E **97**(3), 030201(R) (2018)
27. V.S. Zykov, N. Oikawa, E. Bodenschatz, Selection of spiral waves in excitable media with a phase wave at the wave back. Phys. Rev. Lett. **107**, 254101 (2011)
28. V.S. Zykov, E. Bodenschatz, Stabilized wave segments in an excitable medium with a phase wave at the wave back. New J. Phys. **16**, 043030 (2014)
29. N. Oikawa, E. Bodenschatz, V. Zykov, Unusual spiral wave dynamics in the Kessler-Levine model of an excitable medium. Chaos **25**, 053115 (2015)
30. V.S. Zykov, E. Bodenschatz, Continuous transition between two limits of spiral wave dynamics in an excitable medium. Phys. Rev. Lett. **112**, 054101 (2014)